

J. Environ. Treat. Tech. ISSN: 2309-1185

Journal web link: http://www.jett.dormaj.com



# Detection of Hydrothermal Alteration Zones using Image Processing Techniques, Chahr Gonbad, Iran

Abbas Ali Nouri<sup>1</sup>, Rasoul Sharifi Najafabadi<sup>2</sup>, Mohammad Ali Nezammahalleh<sup>3</sup>\*

PhD Candidate in geomorphology, Kharazmi University, Tehran, Iran Assistant Professor of Geomorphology, Farhangian University, Tehran, Iran PhD in geomorphology, University of Tehran, Tehran, Iran

#### Abstract

Use of satellite images to detect hydrothermal alteration zones can be helpful for efficient mineral explorations. Remote Sensing (RS) techniques make it possible to save cost and time for accurate primary explorations. The purpose of this research is to use the image processing techniques to detect porphyry copper minerals through the index of hydrothermal alteration mapping in Chahr Gonbad, Sirjan, Iran. We have obtained Landsat imagery data of Enhanced Thematic Mapper (ETM) and Operational Land Imager (OLI) for the analysis. For enhancement and detection of the alteration zones, we have applied useful RS methods including image difference and band color composite, band ratios, Principal Component Analysis (PCA), Crosta, and Matched Filtered. The results discovered argillite and propylitic alteration zones through iron-oxide and hydroxyl minerals in the study area. The image processing has revealed that the detected alteration minerals have relation with mineralization of porphyry copper. The zones are mainly developed in a northwest-southeast orientation and mostly concentrated in center and south of the Chahr Gonbad.

Keywords: Porphyry copper, Band ratio, PCA, Crosta, hydrothermal alteration mapping, Chahr Gonbad

## 1 Introduction

Formation of mineral reserves is a complicated geological process (1). Mining engineers and geologists have classified a variety of processes forming mineral materials (2). Hence, the evidence of a variety of minerals is greatly acknowledged and applied in mining explorations (3). Today, the science of remote sensing (4) by many helpful capabilities in processing of satellite images is very important in earth science studies (5-8) including mining explorations, recognition of rock material in geology, detection of faults, mapping, and creating Digital Elevation Model (DEM). The most important advantage of this technique is to have access to essential information in a minimum of time. Since satellite images have spectral data in all ranges of electromagnetic spectrum, they provide useful information about the nature of land surface features. Another advantage of the data is appropriate repetition of imaging that make it possible to investigate geodynamic phenomena (9). The fundamental of these data is based on remotely measuring reflection of the earth features. Hence, it is possible to recognize earth surface features and objects without any direct contact (10).

**Corresponding author:** Mohammad Ali Nezammahalleh, PhD in geomorphology, University of Tehran, Tehran, Iran, Email: mnezammahalleh@ut.ac.ir, Tele: +989108350107.

Ore deposits are geologic 3-dimensional features that include unusual concentration of one or more elements. They are predominantly differentiated from surrounding areas. Exploration of mineralization is based upon use of exceptional conditions in 4 factors including elements, mineralization, petrology, and structure. To make this work, in exploration simplified models of mineralization and metallization are used in some steps.

Porphyry ore deposits can mainly indicate mineralization and alteration zonations (11, 12). Most of the copper porphyry minerals have a distribution pattern resulted from mineralization and alteration of deposits (6, 13). This distribution pattern of hydrothermal alteration zones can be used as an index to enhance and explore the copper porphyry minerals using RS techniques (14, 15, 7). In the recent years, it has been attempted to use spectral characteristics of satellite images in alteration zones and to employ different methods of image processing the alteration mapping (12).

In this research, it has been attempted to use different techniques to discriminate alteration zones with regard to previous studies and lithologic characteristics of the region in order to show promising areas for exploration of porphyry copper.

## 1.2 Geographic and geologic position of Chahr-Gonbad

The study area of this research is Chahr-Gonbad (from 56° 28′ E to 56° 08′ E and from 29° 25′ N to 29° 40′ N), Kerman, Iran. In geologic map, the study area is located in south part of central Iran on Urmia-Dokhtar geologic zone, a metamorphic formation rich in cropped porphyry copper and iron. There are plenty of villages linked by a good transportation network in this mountainous region. Kerman metallogenic belt is south part of the magmatic-metallogenic unit of Urmia-Dokhtar zone and divided into two sections of

Anar-Baft and Baft-Bam. This contains 95% of discovered reserves of copper in Iran. Deposit generation models discuss forming process of a deposit or a mineralization zone as well as examine activating, transporting, and concentrating forces on the elements. A set of the models as conceptual bases for exploration-geologic data may be simultaneously selected for analysis. Although main potential in the region of Anar-Baft metallogenic belt is porphyry copper, but it is also important for vein copper mineralization, poly-metal and vein lead and zinc. (Figure 1).

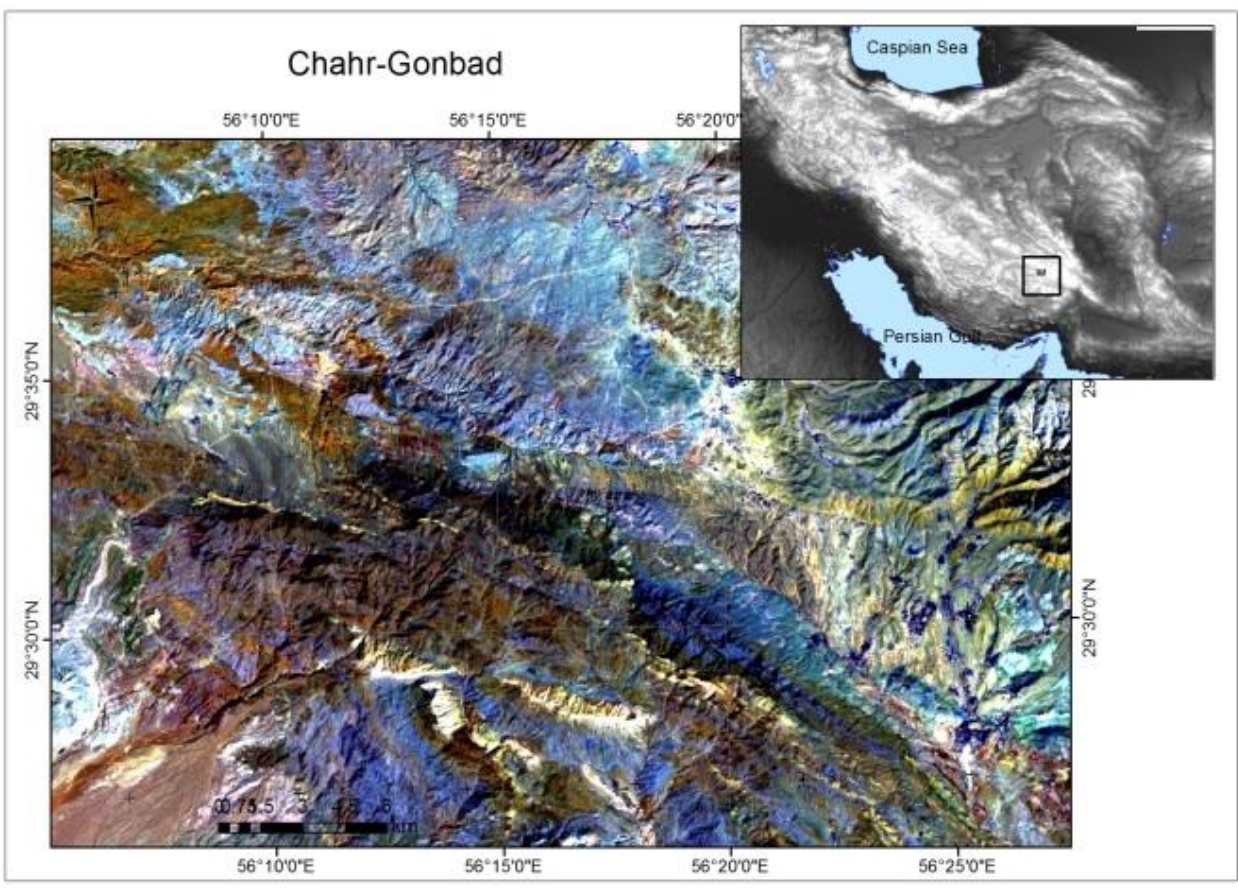


Figure 1: location of the study area

## 2 Materials and method

## 2.1 Processing the region image

We have used Landsat 7 and 8 images captured by Enhanced Thematic Mapper (ETM) sensor in eight bands and Operational Land Imager (OLI) in 7 bands for surveying and exploring hydrothermal alterations of porphyry minerals (16, 17, 18). The study area is located in a scene with path 160 and row 40 of the satellite image. The orthorectified ETM and OLI images of the study area for the date July 22, 2003, and June 1, 2019, with 0% of cloud cover has been taken from Landsat.org. Its geometric precision has also been controlled by topographic map. To eliminate atmospheric effects including water vapor and aerosols, we have used black targets like mountain shadow.

# 2.2 Spectral response of hydrothermal alterations and detection of the minerals on etm+ and oli images

The minerals of hydrothermal alteration zones can be detected on a special range of electromagnetic spectrum mainly in visible and near-Infrared. Because of wide bandwidth of the electromagnetic spectrum of ETM+ and OLI images, they are not able to discriminate separate minerals (16). Nevertheless, they can easily discriminate the minerals in hydrothermal alteration zones in near and middle infrared.

The minerals characterizing the hydrothermal alteration are usually applied in exploration of different minerals, particularly porphyry, using satellite images. These minerals are grouped into three categories: hydroxyl (mica and clay), sulfate dihydrate (gypsum and alunite), and iron-bearing hydroxyl or ferrous minerals (Hematite, Geothite, Jarosite). The minerals mainly detectable in infrared range are belonging to hydroxyls and sulfates. The iron-oxide is often found in alteration zones and surface outcrops due to weathering. Thus, it can be important as a key to show the areas capable of mineralization. The existence of the iron oxide in rocks makes them red, brown, and orange in color. Existence of clay minerals gives light color to the rocks (19). (Figure 2).

Remote sensing techniques have been used for many years to produce the alteration mapping. Today, common image processing techniques are also applied for enhancement and detection of alteration zones. All the data and methods have been employed as supplementary to better find the promising areas in Zone 4, Chahr Gonbad, as the most important porphyry copper in Iran.

## 2.3 Image difference and band color composite

Giving one of the three colors of red, green, and blue to a combination of three bands creates color composite image. There are many studies about the best selection of the colors to show maximum information of the minerals (16). The goal of selecting suitable combination of the bands to produce colored images is to minimize the nonsignificant information and maximize use of valuable information. One method of selecting the color composite is Optimized Index

Factor (OIF).

#### 2.4 Band ratios

The ratios of bands are obtained by dividing DNs in one spectral band by those related to another band in each pixel. The new image is produced as the ratio of values of one band to those of another. One advantage of the ratio images is that they represent the color and spectral characteristics of earth surface features regardless of luminance effects due to various topographies. Indeed, they have no albedo effects of the primary data (20). Remote sensing techniques using the band ratio images have been used for enhancement of hydrothermal alteration zones as well as vegetation covers in many studies (14, 15, 13, 3).

We have tested different band ratios in this study to enhance hydrothermally altered rocks and lithological units. The combinations of bands are selected based on spectral reflectance and position of the absorption bands of the minerals going to be mapped. The following band ratios are usually used for geological use to discriminate lithological features (16). The band ratios are 4/2 for iron oxide, 6/7 for hydroxyl bearing rock, and 7/5 for clay minerals. We have presented the laboratory spectral signatures of some minerals (Figure 3). Dependent on the spectral characteristics of the minerals, we can use band ratios of 3/1 and 5/7 in ETM data to detect iron-oxide and hydroxyl minerals, respectively.

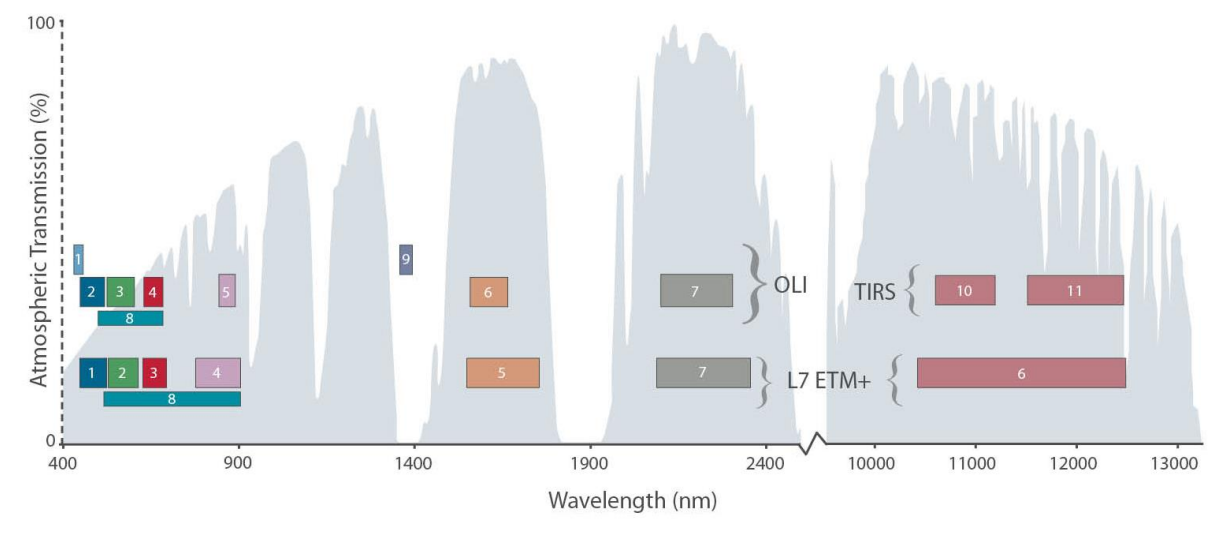


Figure 2: Spectral range of sensors ETM+, OLI, TIRS according to Landsat Website

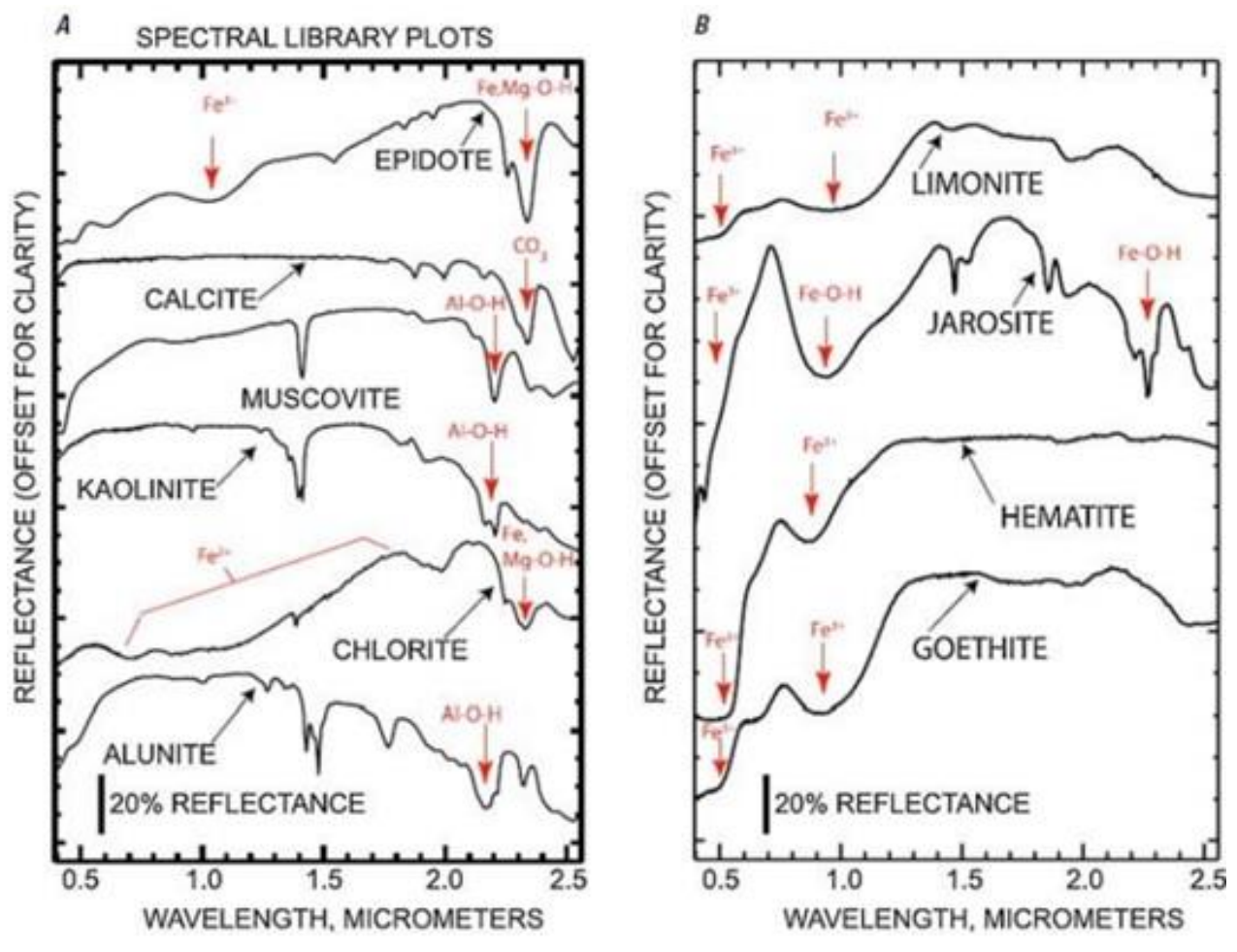


Figure 3: (A) Laboratory spectra of alunite, chlorite, kaolinite, muscovite, calcite, and epidote. (B) Laboratory spectra of limonite, jarosite, hematite and goethite (Beiranvand Pour; 2015).

# 2.5 Standard Principal Component Analysis (PCA) and Crosta

In a look at different bands of a satellite image, e.g., ETM+ and OLI, they seem very similar. This similarity is resulted from correlated information in the bands. Processing of the highly correlated bands is usually difficult in multi-spectral images. There is a great proportion of redundant information in different bands of one image. Rendering the bands uncorrelated helps us to compact the useful information in the multi-spectral images. Using the PCA, we can remove or reduce the redundant information and compress them into a coordinate system without any loss of information. In the analysis, the first principal component explains the highest variance of the data. The main application of the PCA is to reduce the variables called dimensionality reduction. (21)

Using the PCA method, we can examine eigenvector loadings of multi-spectral images to discover the spectral signature of the minerals covered in an image. This is called Crosta technique as a simple way for alteration mapping by Landsat images. Combination of the PCA and Crosta has been applied by many studies for the detection of alterations in metallogenic belts (13). We have used 6 bands including

visible and middle-Infrared bands for the purpose.

## 2.6 Matched filtering

The Matched Filtering (MF) is a technique increasing reference member and minimizing reflectance of undefined background (22). However, all the methods for alteration mapping have a distinction function attempting to discriminate alteration minerals using a certain algorithm. In MF, we initially received the corrected bands and then as another input we integrated that with the spectral signature of the minerals going to be discriminated. We have compared the net spectrums of the minerals from spectral library with the spectrums of the same minerals of this study area. The highest spectral coincidence of the minerals with the library is considered as a recognized class.

## 2 Results and discussion

The results of color composite of the bands 1, 3, 5 of Landsat ETM+ and OLI can give us a clear look of the alteration zones of the region. The Figure 4 shows color composite of the bands 1, 3, 5 of Landsat ETM+ and OLI. In this figure, the alteration zones are showed as white and yellow. Differential band composite of OLI sensor as (2-4)

(3-5) (7-6) by RGB can also well show the alteration zones as illustrated in orange and pink color in Figure 5. The vegetation in red color is discriminated from alteration zones. The results of the band ratios are not clear for ironoxide and not able to discriminate solely the hydroxyl minerals from vegetation. The band ratios of 3/1 and 4/2 show iron-oxide areas and band ratios of 5/7 and 6/7 show hydroxyl areas in the region. In Figure 6, the alteration minerals are represented in white color pixels. For OLI data we can also use band ratio 4/2 for iron-oxide and 7/6 for hydroxyls. Results of the PCA in eigenvectors and eigenvalues of the images related to Chahr-Gonbad in 6 bands of ETM+ have revealed that which of the spectral characteristics of the rocks, vegetation, and soil can account for the statistical variance of the PCs in the region (Table 1). The first PC with a positive weight contains 91% of the variance of ETM+. The remarkable brightness of the region represents high correlation among the 6 bands. The PC2 indicates that visible bands of the eigenvector have negative sign and Infrared bands have positive sign. In fact, the second PC is indicative of the differences between the visible and middle Infrared bands. Therefore, it is expected that materials with the highest spectral reflectance in visible spectrum are appeared in dark color and the materials with the highest spectral reflectance in middle Infrared spectrum are appeared in light color. In PC3 the highest eigenvector is related to the band 4. This indicates that in the PC vegetation is dominant feature of the surface.

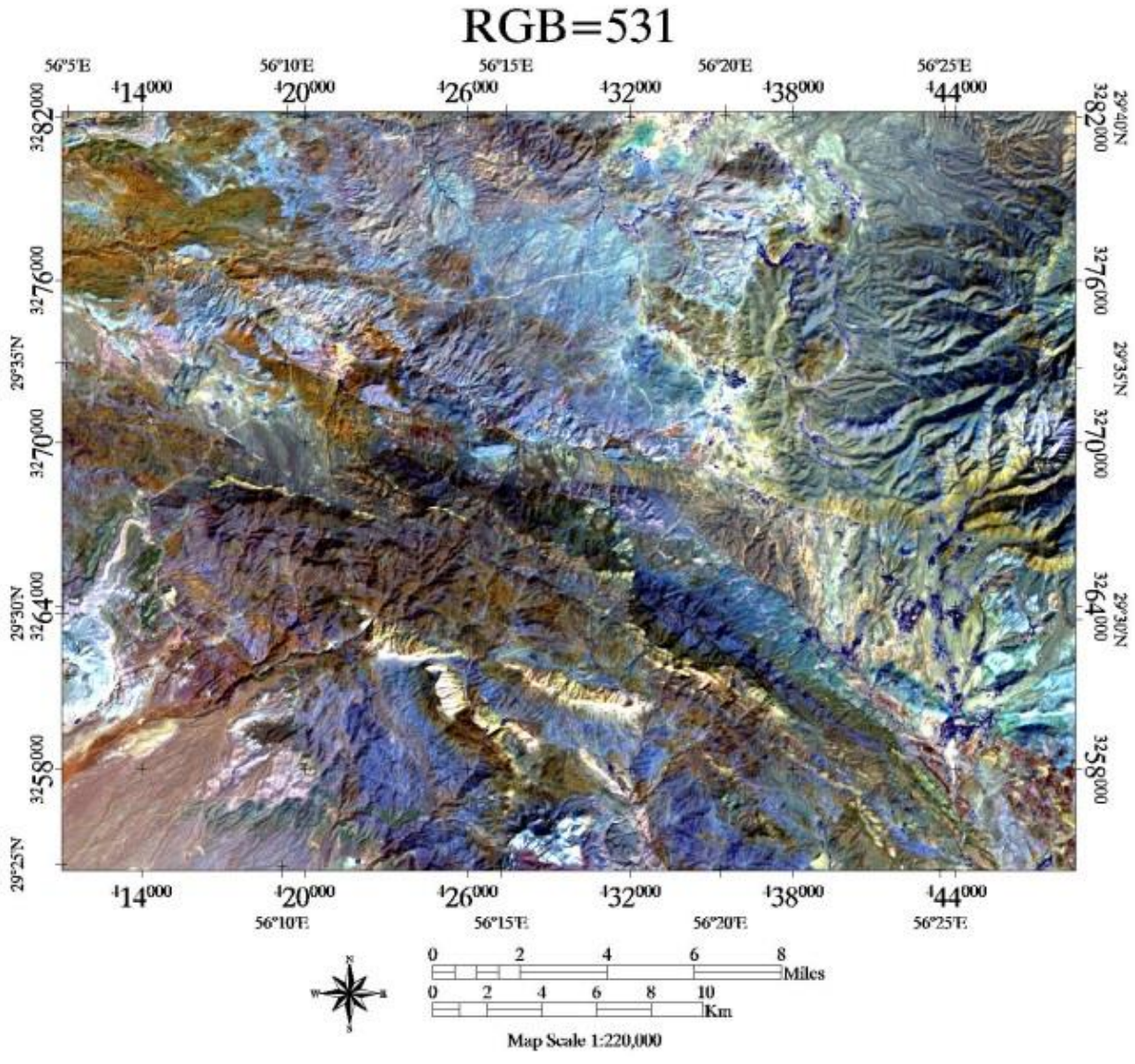


Figure 4: Color composite of the bands 1, 3, 5 of ETM+

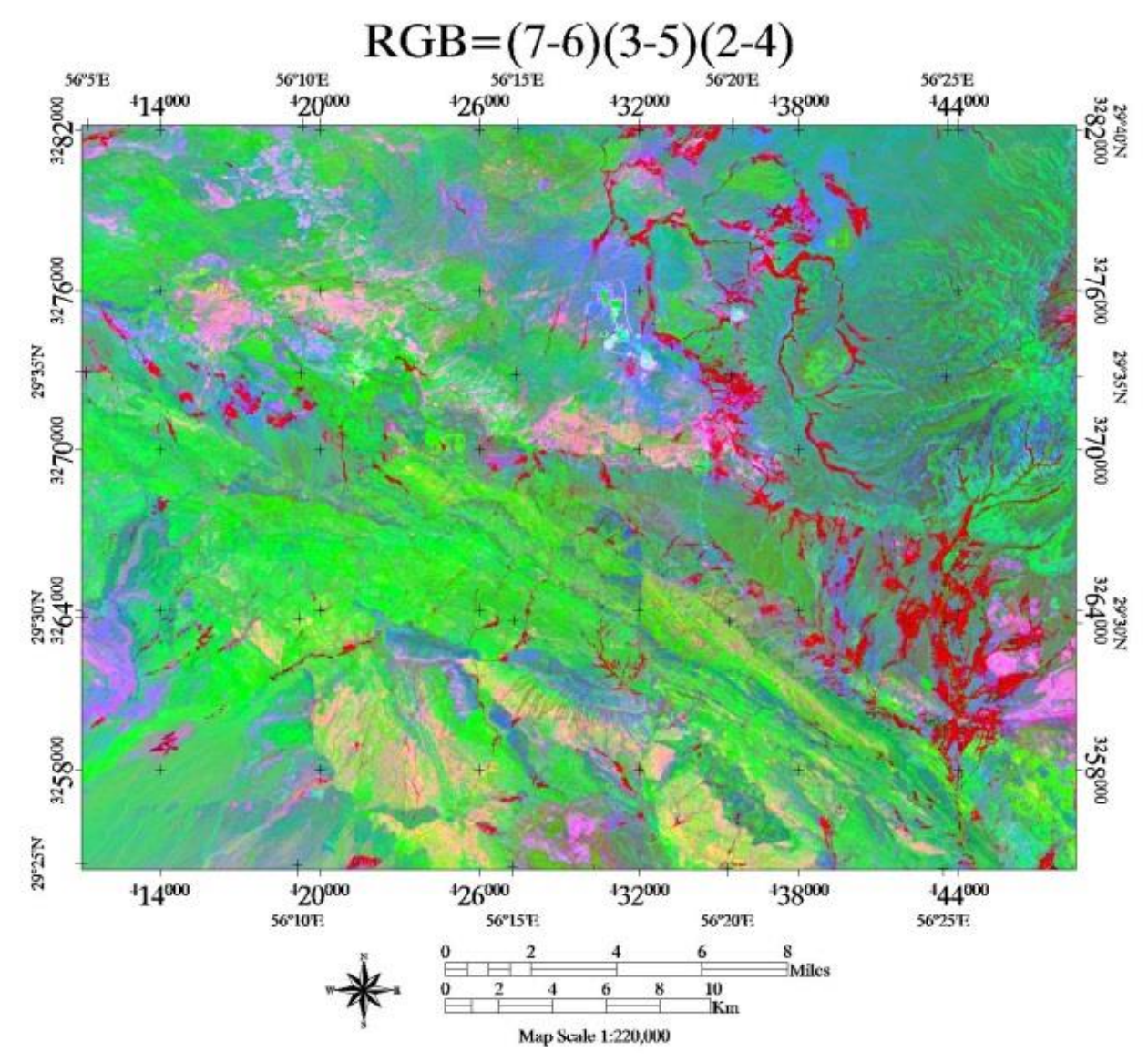


Figure 5: Differential band composite (2-4)(3-5)(7-6) of OLI

The spectral information of clay and iron-oxide in principal components of ETM+ are mainly concentrated in PC5 and PC4. The PC4 with high loadings and opposite sign is discerned in bands 5 and 7. In the band 7 the hydroxyls have high absorption with loadings of -0.668 and in band 5 the minerals have high reflectance with loadings of 0.625. Thus, in PC4 the hydroxyl zones can be seen in light color pixels.

The results of the PCA method in 6 bands of visible and non-thermal infrared of ETM+ indicate that hydroxyls and iron-oxide can be mapped in PC4 and PC5, respectively. In PC5 band 1, in which iron-oxide shows higher absorption, has positive loadings of 0.612 and band 3, in which the mineral shows higher reflectance, has negative reflectance of - 0.686. Thus, the iron-oxide zones are appeared in dark color pixels in PC5.

Table 1: Results of PCA in 6 bands of ETM+ of the study

area						
Eigenvector	Band 1	Band 2	Band 3	Band 4	Band 5	Band 7
pc 1	0.191219	0.284945	0.446248	0.375444	0.559546	0.478597
pc 2	0.458172	0.408835	0.502328	0.034354	-0.52169	-0.31187
pc 3	0.122145	0.102285	0.158869	-0.89479	0.053124	0.38199
pc 4	0.188382	0.250972	-0.12651	-0.21635	0.625795	-0.66865
pc 5	0.612015	0.243922	-0.68638	0.10204	-0.09056	0.276067
pc 6	0.573188	-0.78658	0.190193	0.000119	0.110042	-0.06679

We have used PC5 to show the iron-oxide as light color pixels. (Figure 7). We have combined the three images of principal components by RGB to produce a colored image. We have used PC4 for hydroxyl mapping, PC4+PC5 for hydrothermal alteration mapping, and PC5 for iron-oxide

mapping. The alteration areas have been displayed as white, light blue, and yellow (Figure 8).

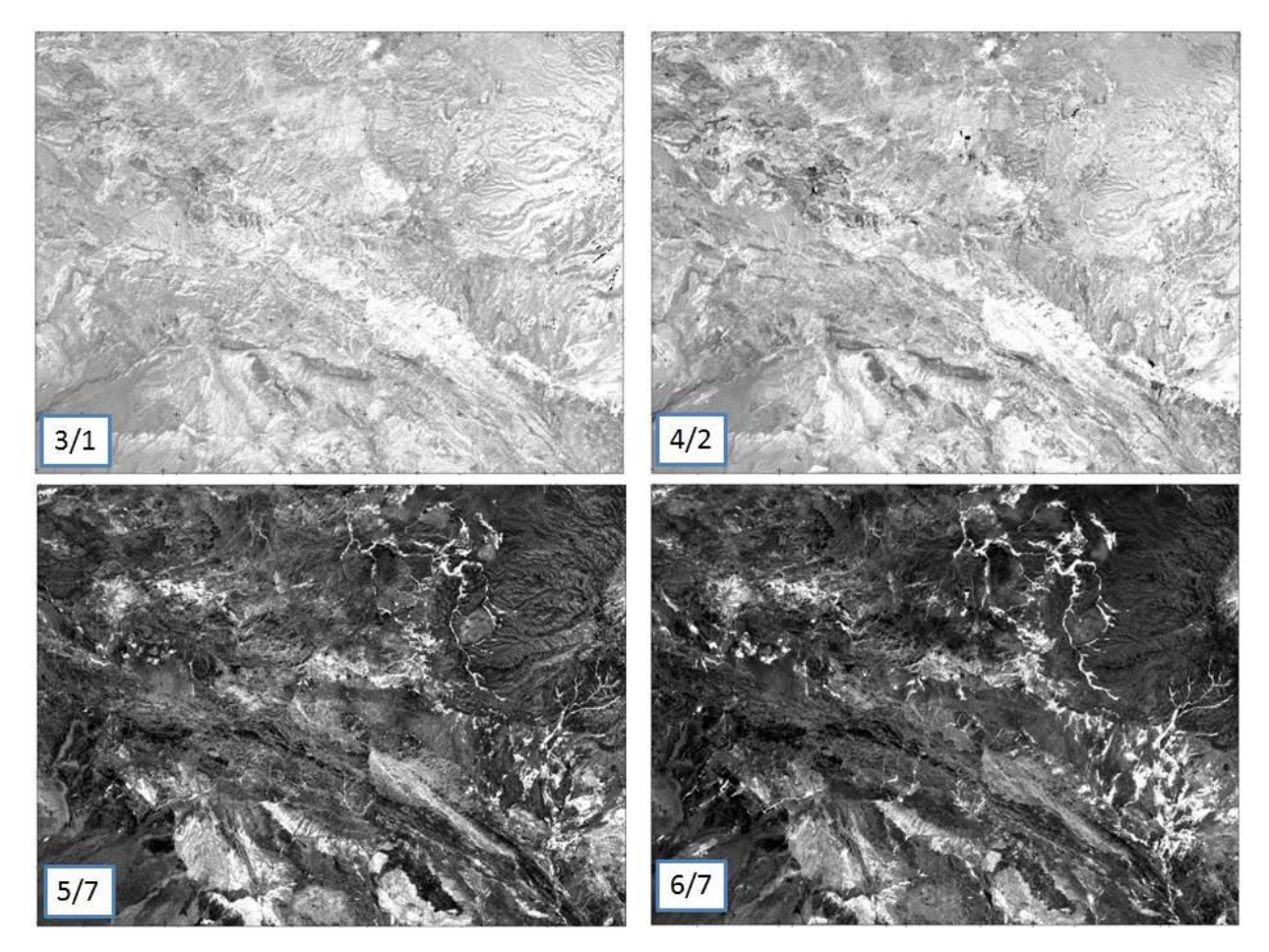


Figure 6: Band ratios 3/1 and 4/2 as well as 5/7 and 6/7 for detection of iron-oxide and hydroxyl

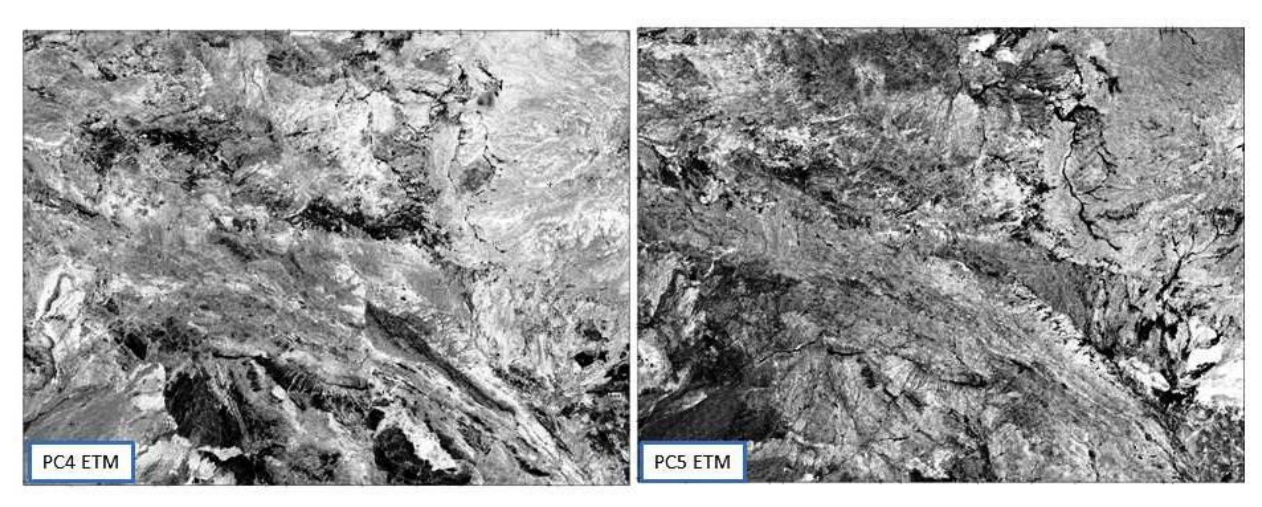


Figure 7: Hydroxyl minerals (light color pixels) in PC4 and iron-oxide minerals (light color pixels) in PC5

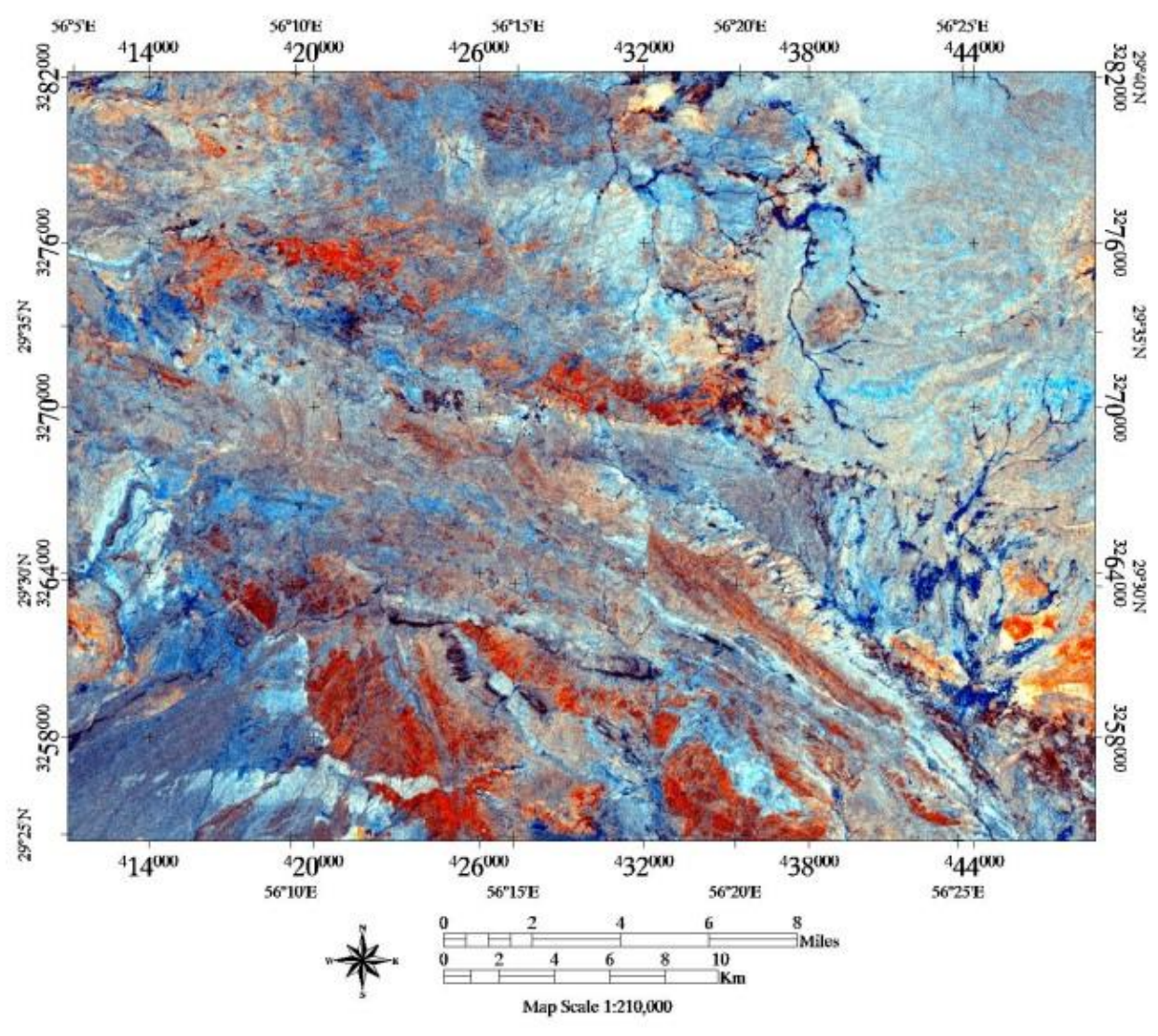


Figure 8: Colored RGB image (PC4, PC4+ PC5, PC5), alteration zones can be seen in white, light blue and yellow

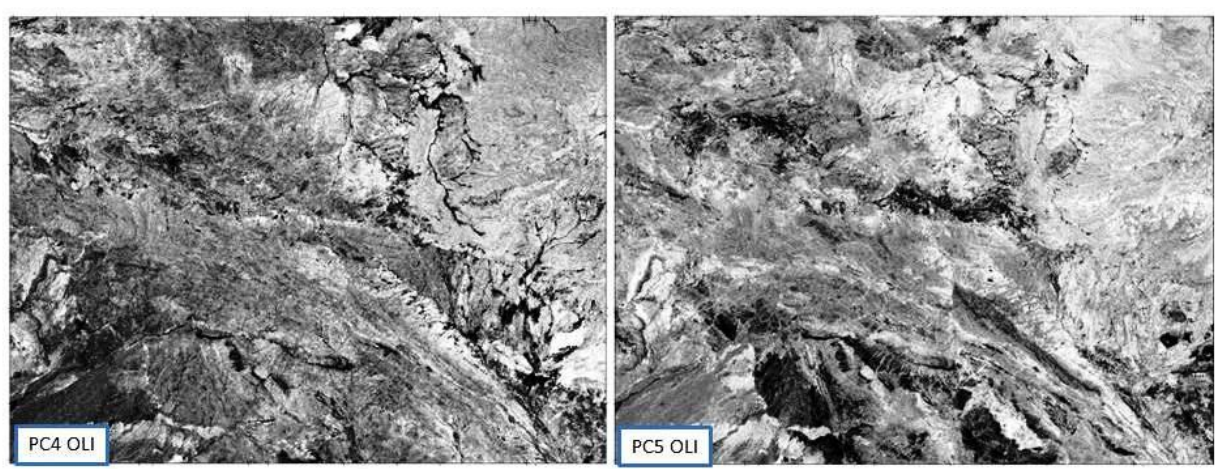
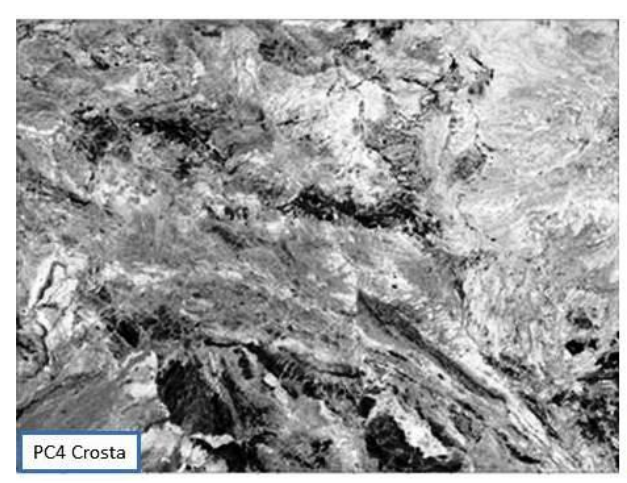


Figure 9: PC4 for hydroxyls (dark pixels and PC5 for iron-oxide (light pixels)



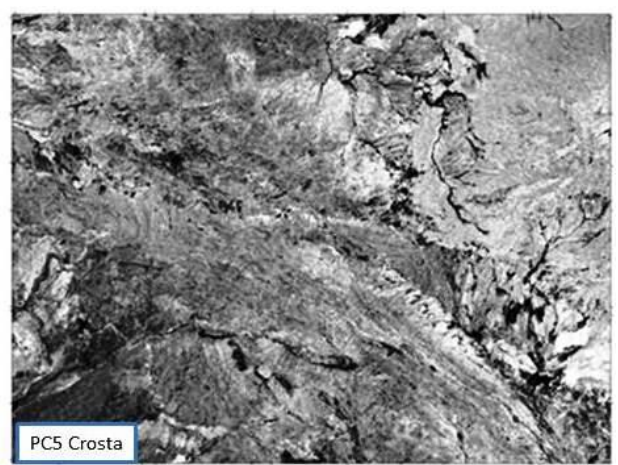


Figure 10: PC4 for iron-oxide minerals (light pixels) and PC5 for hydroxyl minerals (dark color)

Table 2 presents the results of PCA for 7 bands of OLI. PC4 show the highest value for clay minerals in bands 7 and 6. Thus, we can see the clay minerals in dark color in this PC4. In PC5, the iron-oxide in bands 2 and 4 has the highest difference and appeared in light color. (Figure 9)

Table 2: Principal Component Analysis on 6 bands of OLI in the study area

Eigenve ctor	Band 1	Band 2	Band 3	Band 4	Band 5	Band 6	Band 7
pc 1	0.169151	0.190028	0.281966	0.367625	0.400881	0.561398	0.494723
pc 2	0.278427	0.275949	0.253194	0.336229	-0.80084	-0.0812	0.145721
pc 3	0.355453	0.338222	0.294993	0.27665	0.42715	-0.50134	-0.40238
pc 4	0.031524	0.041522	-0.13226	-0.14763	0.120777	-0.61162	0.754539
pc 5	-0.46597	-0.41025	-0.04982	0.753404	0.01983	-0.20981	0.007469
рс 6	0.366918	0.177897	-0.85826	0.292869	0.022597	0.093206	-0.04633
pc 7	0.644026	-0.75609	0.113067	-0.00913	0.000739	-0.01062	0.024011

In the Crosta selective PCA method, we have applied the

appropriate bands of high information, for example, near infrared (VNIR) for iron-oxide and shortwave infrared (SWIR) for argillite and propylitic zone. Reducing the number of bands in PCA ensure that some features are excluded to better find some special features of interest. This technique called Crosta makes it more likely to discover the minerals of the study. We have conducted two PCAs in this research. In one analysis, we included bands 1, 3, 4, and 5 for extraction of iron-oxide and excluded band 7 to prevent hydroxyl mapping. In the other analysis, we included bands of 1, 4, 5, and 7 for extraction hydroxyl minerals and excluded bands 2 and 3 to prevent iron-oxide mapping (Table 3). All statistical information including eigenvector, correlation matrix, and eigenvalues have been analysed for both the groups of bands. Given the higher spectral reflectance of iron-oxide in band 3 and higher absorption in band 1 along with the coefficients of eigenvectors, the areas spotted by the iron-oxide are discriminated by light color on PC4 (0.673 and -0.722) (Figure 10 and 11). The higher spectral reflectance of hydroxyl minerals in band 4 and higher absorption in band 7 along with the coefficients of the eigenvectors are discriminated the areas spotted by hydroxyl as dark color on the PC4 (0.670 and -0.609) (Figure 12). (Table 4).

Table 3: eigenvector of PCA for iron-oxide

Eigenvector	Band 1	Band 3	Band 4	Band 5
PC 1	-0.21433	-0.43232	-0.56632	-0.66816
PC 2	-0.48179	-0.4385	-0.30336	0.695393
PC 3	0.447459	0.408431	-0.75974	0.236137
PC 4	-0.7223	0.673795	-0.10026	-0.11929

Table 4: eigenvector of PCA for hydroxyls

Eigenvector	Band 1	Band 4	Band 5	Band 7
Band 1	-0.1875	-0.50969	-0.62884	-0.55644
Band 3	-0.28778	-0.78853	0.389394	0.379186
Band 5	0.854177	-0.30267	-0.28541	0.311954
Band 6	-0.39039	0.163824	-0.60949	0.670284

As reference data to recognize iron-oxides and clay minerals, we have compared spectral signature of 7 minerals including Hematite, Geothite, Calcite, Illite, Jarosite, Kaolinite, and Limonite. The references have been received from USGS spectral collection. To compare the existing spectral bands from USGS with OLI and ETM images, the laboratory spectrums need to be resampled for every band of the image. The results of the previous methods show good consistence with this method. (Figure 11).

## 2 Conclusions

Formation of mine reserves as a complicated geologic process is influenced by a variety of environmental factors. Many geologists and mine specialists classified various processes of development of minerals. Hence, the evidence and signs of existence of minerals are well recognized for exploration and mining activities. Given that the alteration mapping can be used as an indicator of exploration, discovering the alteration zones can be very useful for exploration activities in regional level. Using band composite, band ratio, PCA, Crosta and matched filtered methods, we have processed ETM+ and OLI images of Chahr-Gonbad and detected alteration minerals in relation with mineralization of porphyry copper. This is greatly consistent with the findings of Ercan et al. (2016) about the relation of alteration minerals with the mineralization. The results of the analyses have documented that the alterations are mainly argillite and propylitic and that the hydroxyls are mostly concentrated in central, west, and southeast portions of the study area in a southeast-northwest orientation. According to these results, the iron-oxide is also concentrated mainly in southeast and central parts of the study area. Indeed, the exploration results, whether exact, cannot substitute direct observation of geologic features. However, there may be no mineralization in the detected areas or they may not be so economical. Therefore, for evaluation of the resulted areas and discriminating the false anomalies from the real, it is necessary to make a field survey control of the anomalies.

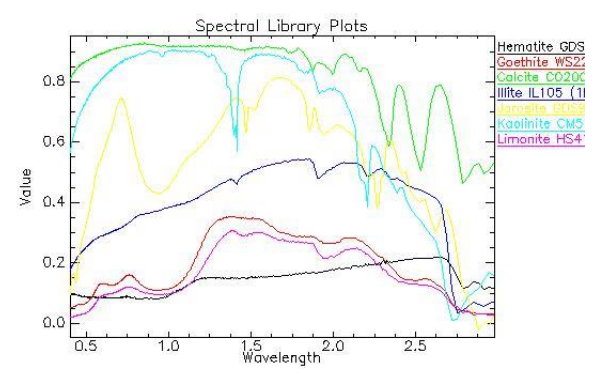


Figure 11: spectral response of the minerals of the study using MF

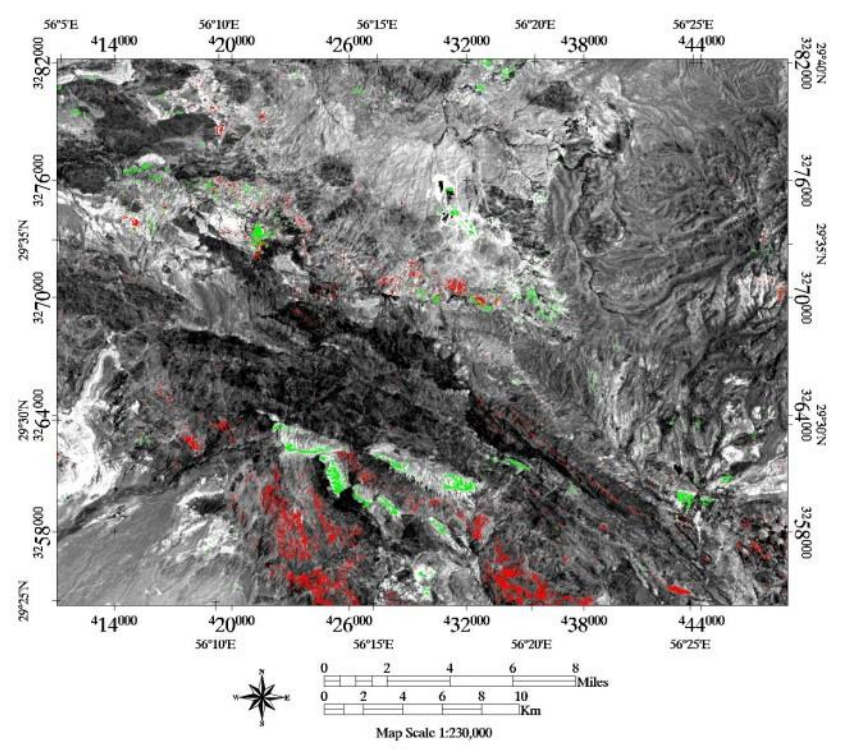


Figure 12: Mapping of iron-oxide areas with red color and clay minerals with green color

# Aknowledgment

The authors are grateful to Hassan Nezammahalleh for providing useful advices for English editions.

## **Ethical issue**

Authors are aware of, and comply with, best practice in publication ethics specifically with regard to authorship (avoidance of guest authorship), dual submission, manipulation of figures, competing interests and compliance with policies on research ethics. Authors adhere to publication requirements that submitted work is original and has not been published elsewhere in any language.

# **Competing interests**

The authors declare that there is no conflict of interest that would prejudice the impartiality of this scientific work.

## Authors' contribution

All authors of this study have a complete contribution for data collection, data analyses and manuscript writing.

## References

- Jiang, Chen; Mahyar Yousefi; Yan Zhao; Chunpeng Zhang; Sen Zhang; Zhaoxia Mao; Mingshen Peng; Renping Han; (2019) Modelling ore-forming processes through a cosine similarity measure: Improved targeting of porphyry copper deposits in the Manzhouli belt, China; Ore Geology Reviews 107, 108-118.
- Tursunai Bektemirova; Apas Bakirov; Ruizhong Hu; Hongping He; Yuanfeng Cai; Wei Tan; Aiqing Chen; (2018) Mineralogical evolution of the paleogene formations in the Kyzyltokoy basin, Kyrgyzstan: implications for the formation of glauconite, Clays and Clay Minerals 66 (1): 43-60
- Ferrier Graham; Athanassios Ganas; Richard Pope, (2019)
   Prospectivity mapping for high sulfidation epithermal porphyry deposits using an integrated compositional and topographic remote sensing dataset; Ore Geology Reviews 107, 353-363.
- Curan, P.J. (1986) Principle of remote sensing; Longman Scientific & Technical, New York, 282.
- Percival, Jeanne B.; Sean A. Bosman; Eric G. Potter; Jan M. Peter; Alexandra B. Laudadio; Ashley C. Abraham; Daniel A. Shiley; Chris Sherry; (2018) Customized Spectral Libraries for Effective Mineral Exploration: Mining National Mineral Collections, Clays and Clay Minerals 66, 297-314.
- (6) Salehi, Touba; Majid H. Tangestani (2018), Large-scale mapping of iron oxide and hydroxide minerals of Zefreh porphyry copper deposit, using Worldview-3 VNIR data in the Northeastern Isfahan, Iran; International Journal of Applied Earth Observation and Geoinformation 73, 156-169.
- Tapia Joseline; Brian Townley; Loreto Córdova; Fernando Poblete; César Arriagada; (2016) Hydrothermal alteration and its effects on the magnetic properties of Los Pelambres, a large multistage porphyry copper deposit; Journal of Applied Geophysics 132, 125-136.
- Rowan, L.C., Mars, J.C., (2003) Lithologic mapping in the Mountain Pass, California area using Advanced Spaceborne Emission and Reflection Radiometer (ASTER) data, Remote Sensing of Environment 84, 350–366.
- Kaufmann, H.J., (1988) Mineral exploration along the Aqaba-Levant structure by use of TM-data-concepts, processing and results, International Journal of Remote Sensing 9, 1639-1658

- Fujisada, H., Iwasaki, A., HARA, S., (2001) ASTER stereo system performance, proceeding of SPIE, the international society for optical engineering, 4540:39-40
- Abrams, M.J., Brown, D., Lepley, L., Sadowski, R., (1983), Remote sensing for porphyry copper deposits in Southern Arizona, Economic Geology 78, 591-604
- Ruiz Armenta, J.R. and Prol-Ledesma, R.M., (1998); Techniques for enhancing the spectral response of hydrothermal alteration minerals in Thematic Mapper images of Central Mexico, International Journal of Remote Sensing 19, 1981-2000.
- Ercan, Hatice Ünal; Ü. Işik Ece; Paul A. Schroeder;
   Zekiye Karacik, (2016) Differentiating Styles of Alteration within Kaolin-Alunite Hydrothermal Deposits of Çanakkale,
   NW Turkey, Clays and Clay Minerals 64, 245-274.
- Rowan, L.C., Goetz, A.F.H. and Ashley, R.P., (1979)
   Discrimination of hydrothermally altered and unaltered rocks in the visible and near infrared: geophysics 42, 533-535.
- Podwysocki, M.H., Segal, D.B. and Abrams, M.J., (1983) Use of multispectral scanner images for assessment of hydrothermal alteration in the Marysvale, Utah mining area, Economic Geology 78, 675-687.
- Beiranvand Pour Amin; Mazlan Hashim; (2015) Hydrothermal alteration mapping from Landsat-8 data, Sar Cheshmeh copper mining district, south-eastern Islamic Republic of Iran; Journal of Taibah University for Science 9; 155-166.
- Bennet, S.A., Atkinson, W.W. and Kruse, F.A., (1993) Use of Thematic Mapper imagery to identify mineralization in the Santa Tersa district, Sonora, Mexico: International Geology Review 35, 1009-1029.
- Chavez, P. S., Kwarteng, A. Y., (1989) extracting spectral contrast in Landsat Thematic Mapper image data using selective principal component analysis. Photogrammetric Engineering and Remote Sensing 53, 339-348.
- Tangestani, M.H. and Moore, F., (2000); Iron-oxide and hydroxyl enhancement using the Crosta method: A case study from the Zagros Belt, Fars province, Iran, Journal of Applied Geosciences 2, 140-146.
- Sabins Rowan, F.F., (1996) Remote Sensing (Principle and Interpretation), W.H.Freeman Co., New York, PP 575
- 21. Crosta, A.P. and Moore, McM., (1989); Enhancement of Landsat Thematic Mapper imagery for residual soil mapping in SW Minais Gerais State, Brazil: A prospecting case history in Greenstone belt terrain, Proceeding of the 7th ERIM thematic conference: Remote Sensing For Exploration Geology, 1173-1187.
- Harsanyi, Joseph C.; Chang, Chein-I; (1994) Hyperspectral Image Classification and Dimensionality Reduction: An Orthogonal Subspace Projection Approach, IEEE Transactions on Geoscience and Remote Sensing 32(4), 779 – 785